Time-lapse three-dimensional electromagnetic inversion of growth-impeded SAGD steam chambers

Sarah G. R. Devriese and Douglas W. Oldenburg*
Geophysical Inversion Facility, University of British Columbia

SUMMARY

Heterogeneity in the Athabasca oil sands can impede the growth of SAGD steam chambers. Here, we show how controlled-source electromagnetic (EM) methods can be used to detect growth-impeded regions and monitor changes in steam chamber growth. Our achievements are two-fold. We first generate a background resistivity model based on well logging at a field site in the Athabasca oil sands and then estimate the resistivity of the steam chambers using an empirical formulation that incorporates the effects of temperature on the surrounding rocks. Using the resulting 3D model, electromagnetic responses for any EM survey can be computed. The second, and more important, achievement illustrates that imaging SAGD chambers, as they grow in time, may be possible with cost-effective surveys. Our example uses a single transmitter loop with receivers in observation wells. In the wells, only the vertical component of the electric field is measured. Even with this limited data set, the images obtained through 3D cascaded time-lapse inversion identifies the location and extent of an impeded steam chamber. The proposed EM survey acquisition time and processing should be relatively fast and cost-effective, and are expected to yield sufficient information to help make informed decisions regarding SAGD operations.

INTRODUCTION

Steam Assisted Gravity Drainage (SAGD) is an in-situ recovery process used to extract bitumen from the Athabasca oil sands in northeast Alberta. In SAGD, two horizontal wells are drilled at the bottom of the reservoir (Dembicki, 2001). Steam is injected into the top well and produces a steam chamber that grows upwards and outwards. At the edge of the chamber, the heated, fluid oil and condensed water flow through the formation and are collected by the underlying horizontal production well. The chamber expands further into the bitumen reservoir as the oil drains (Butler, 1994).

The success of this technique is dependent upon steam propagation throughout the bitumen reservoir. However, reservoir heterogeneity, such as clay beds and mudstone laminations, can cause low-permeability zones that can impact the growth of the steam chambers (Strobl et al., 2013; Zhang et al., 2007). This affects the amount of produced oil and exemplifies the importance of monitoring the steam chamber growth. Successful monitoring can aid in optimizing production efforts by increasing understanding of the reservoir, decreasing the steam-to-oil ratio, locating missed pay, identifying thief zones, and more efficiently using resources (Singhai and Card, 1988).

Because the electrical conductivity of a lithologic unit is affected by steaming, electric and electromagnetic methods are promising tools to detect and image SAGD steam chambers. Additionally, these types of surveys can be much more cost-effective than seismic methods (Engelmark, 2007; Unsworth, 2005). Electric and electromagnetic surveys can also be readily installed as permanent installations. Tøndel et al. (2014) used a permanent electrical resistivity tomography (ERT) installation in the Athabasca oil sands to monitor SAGD steam chamber growth over time. From their study, electrodes can stand up to the high-temperature environment in boreholes surrounding the steam chambers while geophones can break down over time. Devriese and Oldenburg (2015) showed how the method can be extended to frequency- and time-domain EM. Permanent installations can also provide multiple data sets per year, without being limited by access to the area in wintertime only.

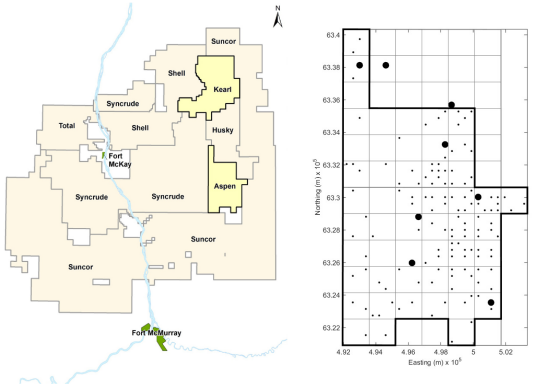

(a) (b)

Figure 1: (a) Map showing properties and their respective companies. The Aspen property, owned by Imperial Oil, is located roughly 45 NE of Fort McMurray and 25 km SE of Fort McKay in northeastern Alberta. Figure courtesy of Imperial Oil. (b) The eight wells used in this paper are indicated by large dots while other wells are shown as small dots. The map shows the boundary of the Aspen Property, boundaries for Townships 93 and 94 in Range 7, and the sections within those townships.

In this paper, we investigate the use of controlled-source EM to recover multiple steam chambers in a well pad at different time-steps. The growth of one of the chambers has been impeded by heterogeneous blockages in the reservoir. A 1D resistivity model is built based on resistivity well logging at a field site in the Athabasca oil sands. We use EM to detect the resistivity changes due to SAGD and recover the chambers using time-lapse 3D inversion.

FIELD SITE

The Aspen property is owned by Imperial Oil and is the future site of several SAGD well pads. The project area lies about 45 km northeast of Fort McMurray and 25 km southeast of Fort

DOI http://dx.doi.org/10.1190/segam2015-5909921.1

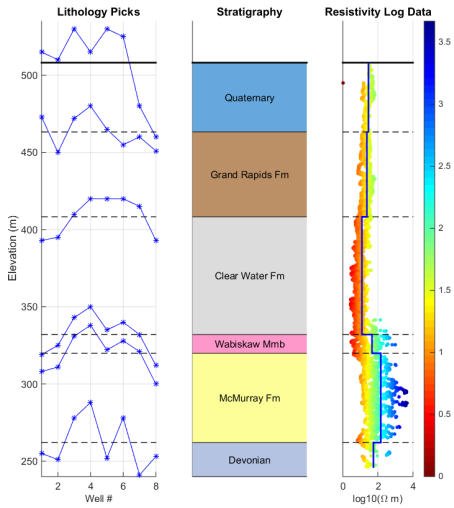

Figure 2: (a) For each of the 8 wells, the top of each lithologic unit was picked. (b) The elevations of the picks were averaged to get a single stratigraphic column of the different units. (c) The resistivity logs from the eight wells are plotted together. For each unit, the average resistivity (plotted in blue) is chosen as a single resistivity for that lithology unit.

MacKay in northeastern Alberta, Canada. Figure 1(a) shows the Aspen property in relation to the two towns and the other properties in the area. Many vertical wells have been drilled on and around the Aspen property (Imperial Oil Resources Ventures Limited, 2013). Since many of these are publicly available, we use eight vertical wells that contain resistivity logging and lithology picks for this research (Wynne et al., 1994). Figure 1(b) shows the location of these eight wells along with the other wells within the property.

1D RESISTIVITY MODEL

We first gather the resistivity log data from the eight wells shown in Figure 1(b). Based on the lithology, horizons are added for the tops of the overlying Quaternary units, the Grand Rapids Formation, the Clearwater Formation (including the Wabiskaw Member), the McMurray Formation, and the underlying Devonian units (Wynne et al., 1994; Imperial Oil Resources Ventures Limited, 2013). The lithology picks, stratigraphic column, and resistivity log data are shown in Figure 2. For each lithologic unit, the resistivity logging data are averaged to generate a semi-synthetic one-dimensional resistivity model for the Aspen property. The 1D model is overlain on the resistivity logging data in Figure 2(c).

WAXMAN-SMITS EQUATION

Resistivity can be estimated reasonably well using empirical formulations. The most well-known is Archie's law, which is an empirical formulation for the resistivity of clean sands:

$$\frac{1}{\rho} = \sigma = \frac{\phi^m s^n \sigma_w}{\gamma}, \tag{1}$$

where ρ is the resistivity, σ is the conductivity, ϕ is the porosity, m is the cementation exponent, s is the water saturation, n is the saturation exponent, σ_w is the water conductivity, and γ is the tortuosity. Note that resistivity is inversely proportional to conductivity.

However, Archie's law does not adequately represent the conductivity changes due to steaming in oil-rich sands (Mansure et al., 1993). Formulations such as the Waxman-Smits equation and the dual-water model are superior because they incorporate the behavior of clays and the bound-water interactions, respectively. Given the available data, we use the Waxman-Smits equation to model the conductivity changes due to SAGD in the Athabasca oil sands. The Waxman-Smits equation (Waxman and Smits, 1968; Waxman and Thomas, 1974; Mansure et al., 1993) is written as following:

$$\sigma = \frac{s^n \left(\sigma_w + \frac{BQ_v}{s}\right)}{F^*}, \tag{2}$$

where B is the specific counter-ion conductance and Q_v is the cation exchange capacity. The water conductivity $\sigma_w = c(T + 21.5)$ is dependent on salinity c and temperature T. The shaley-sand formation factor F^* is expressed as

$$F^* = \frac{\gamma}{\phi^m}\left(1 + \frac{BQ_v}{\sigma_w}\right). \tag{3}$$

The specific counter-ion conductance B can be further written as

$$B = 3.83(0.04T)(1 - 0.83exp(-0.5\sigma_w|_{T=25})). \tag{4}$$

Additionally, the cation exchange capacity is written as

$$Q_v = \frac{V_{cl} C \delta}{\phi}, \tag{5}$$

where V_{cl} is the percentage of clay, C is the cation exchange coefficient, and δ is the density.

At the Aspen property, the oil saturation is approximately 80% for the McMurray Formation with an average porosity of 33% (Imperial Oil Resources Ventures Limited, 2013). Density is reported as 2.65 g/cm^3, the cementation exponent m as 1.8, and the saturation exponent n as 1.7. The background temperature at the Aspen property is 7°C. We used a tortuosity value of 1.63 (Bell et al., 2011).

We assumed a clay volume of 1% and a cation exchange capacity of 0.25 meq/g for the McMurray Formation while 60% and 0.4 meq/g, respectively, for the Wabiskaw Member. Salinities were estimated as 2,460 and 530 ppm for the McMurray Formation and Wabiskaw Member. Applying these parameters in Equations 2-5, we calculate a resistivity of 147 Ωm for the McMurray Formation and 46 Ωm for the Wabiskaw Member. These values match with those from the resistivity well logs.

DOI http://dx.doi.org/10.1190/segam2015-5909921.1

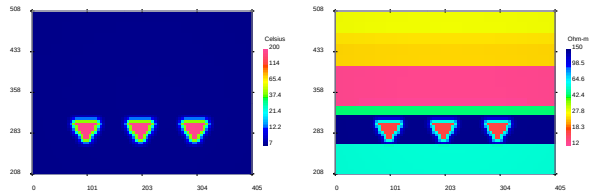

(a) (b)

Figure 3: (a) Cross-section of the 3D temperature distribution within the reservoir for three synthetic steam chambers. (b) Cross-section of the 3D resistivity model based on resistivity log data and the Waxman-Smits equation.

MODELING STEAM CHAMBERS

We adapt the formulation by Reis (1992) to generate a series of steam chambers:

$$W_s = tH\sqrt{2/a}, \tag{6}$$

where W_s is the half-width of the steam chamber, H is the vertical distance between the top of the steam chamber and the producing well, $a = 0.4$ is a dimensionless temperature coefficient, and $t = 0.25$ is a dimensionless time since production started. This example uses three chambers with a height of 35 m. Each chamber is 400 m in length and is separated by 100 m at the base.

In SAGD processes, we expect that the temperature, salinity, and saturation will change due to steaming. We assume that the changes due to salinity and saturation are limited to the extents of the steam chamber. For this investigation, salinity and saturation are kept constant over time. Temperature will radiate outwards from the steam chamber and thus alter the conductivity of the surrounding geology. We use the temperature distribution described by Reis (1992) and formulate it as a function of radial distance d from the steam chamber:

$$T(d) = T_0 + (T_s - T_0)e^{-\frac{aUd}{\alpha}}, \tag{7}$$

where T_0 is the initial reservoir temperature, T_s is the steam temperature, U is the steam front velocity, and α is the temperature diffusivity. The constant $a = 0.4$ is the same as in Equation 6. For this problem, the temperature diffusivity is 0.0507 m^2/day, the steam front velocity is 0.0417 m/day, and the steam temperature is 200°C. Figure 3(a) shows the temperature distribution within the reservoir for the three synthetic steam chambers.

Given the initial resistivity values (Figure 2), we now calculate the resultant resistivity due to the change in temperature using Equations 2-5. Instead of a constant initial temperature, the 3D temperature distribution calculated in Equation 7 is used. The calculated resistivity within the steam chambers is 16 Ωm, which then diffuses back to the background value away from the chambers. A cross-section of the 3D resistivity model is shown in Figure 3(b).

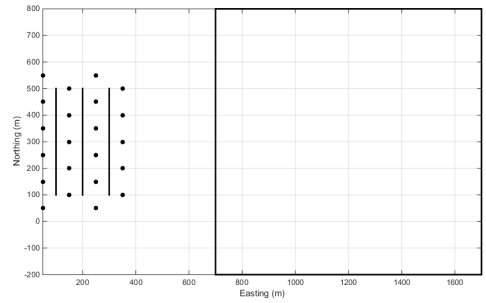

Figure 4: The electromagnetic survey consists of a 1 km by 1 km loop at the surface. The z-component of the electric field is measured at receivers in boreholes (dots) that surround the three horizontal wells (black lines). Each borehole has 33 receivers, spaced every 20 m. Receivers are spaced every 5 m in the bitumen reservoir.

EM SURVEY AND INVERSION RESULTS

Many EM surveys are possible. Inductive or galvanic transmitters can be used on the surface or in boreholes. Receivers can measure three components of electric and/or magnetic fields and they can also be on the surface or in boreholes. Finally, the exciting currents in the transmitter can be at particular frequencies or have an arbitrary time-varying waveform. The ability to detect and resolve resistivity structure depends upon the details of the survey and invariably, more transmitters and receivers located closer to the steam chambers will provide higher-quality information (Devriese and Oldenburg, 2014). Here, we aim to illustrate the potential of using a logistically-simple and cost-effective EM survey. Devriese and Oldenburg (2015) showed that it is possible to excite a steam chamber with a large surface loop carrying harmonic waveforms at different frequencies. Here, we restrict receiver locations to the observation wells that are routinely drilled. The data are the vertical components of the electric field which are measured by installing electrodes down the well. Receivers are placed in 11 observation wells and spaced every 20 m, except in the bitumen reservoir where there are receivers every 5 m. Three frequencies were chosen based on skindepth $D \approx 500\sqrt{\rho/f}$, where ρ is the average resistivity of the layers above the McMurray Formation and f is the frequency. Based on this, we chose frequencies of 10, 50, and 100 Hz.

We add 2% Gaussian noise to the forward modeled EM data and assign uncertainties using a percentage of the data and a noise floor. The steam chambers are recovered using 3D octree inversion (Haber et al., 2012). In this inversion, the background 1D model was used as the initial and reference model. Resistivity changes were limited to the heavy oil reservoir (263 m $< z <$ 318 m). An upper bound was used to limit the highest resistivity to 147 Ωm as the steam is expected to decrease the resistivity. The inversion was run in less than 13 hours on 3 cluster nodes with 24 processors and converged in 11 Gauss-Newton iterations. The result (Figure 5(b)) is compared to the true model (Figure 5(a)). The location and extent of the

DOI http://dx.doi.org/10.1190/segam2015-5909921.1

three chambers are adequately recovered. They appear much smoother than the true model and are not as conductive. However, we can infer that the chambers are growing regularly and no blockages are impacting the flow of steam into the reservoir.

We contrast this scenario with one where a steam chamber is impeded by heterogeneity in the reservoir, causing it to not grow properly (Figure 5(c)). The resistivity is calculated in the same manner as before. We use the same survey and noise parameters to forward model and invert the EM data in three dimensions. The background layered resistivity model is used as the initial and reference model. The inversion reached target misfit in 11 iterations and 13 hours using the same processors as in the previous inversion. The recovered model is shown in Figure 5(d). The inversion shows that the center chamber has impeded growth, indicating the presence of a blockage.

In a final example, Equation 6 is used to generate chambers at a later time, where the chambers are now 50 m in height. The area of impeded growth in the previous example now has a chamber of 20 m in height. The resistivity for this model is calculated as previously discussed and shown in Figure 5(e). EM data are forward modeled in 3D using the survey in Figure 4 and Gaussian noise is added to the data. Here, we use cascaded time-lapse inversion (Hayley et al., 2011), where the initial model is the recovered model from the previous time-step (i.e., the result in Figure 5(d)). Because the later time-step evolves from the previous one, the previously recovered model provides a good starting model for the inversion. All other parameters are kept consistent with the previous inversions. The recovered model, shown in Figure 5(f), shows chambers that are more conductive and larger in volume. The area of impeded growth is now slightly filled in as well.

CONCLUSIONS

We have demonstrated, using a synthetic model, how a SAGD steamed reservoir can be imaged using EM. The survey was limited to a single transmitter at the surface with receivers that measure only the z-component of the electric field in standard observation wells. Data were inverted using cascaded time-lapse inversion and the results illuminated the location of a growth-impeded zone within the steam chamber and showed increased steam saturation at a later time. Data for the simulated survey can likely be acquired in a day, provided that the electrodes are in place in the observation wells. The inversion is straight-forward and readily carried out. The resultant images can be valuable in locating zones with poor steam penetration and serve as a catalyst for carrying out additional EM surveys that can enhance resolution. Such surveys might involve additional transmitters and/or receivers coupled with inversions that incorporate more a-priori information. We are continuing research on these topics with the goal of delineating cost-effective survey designs and inversions that show how EM may provide an effective and practical addition to current monitoring procedures in the Athabasca oil sands.

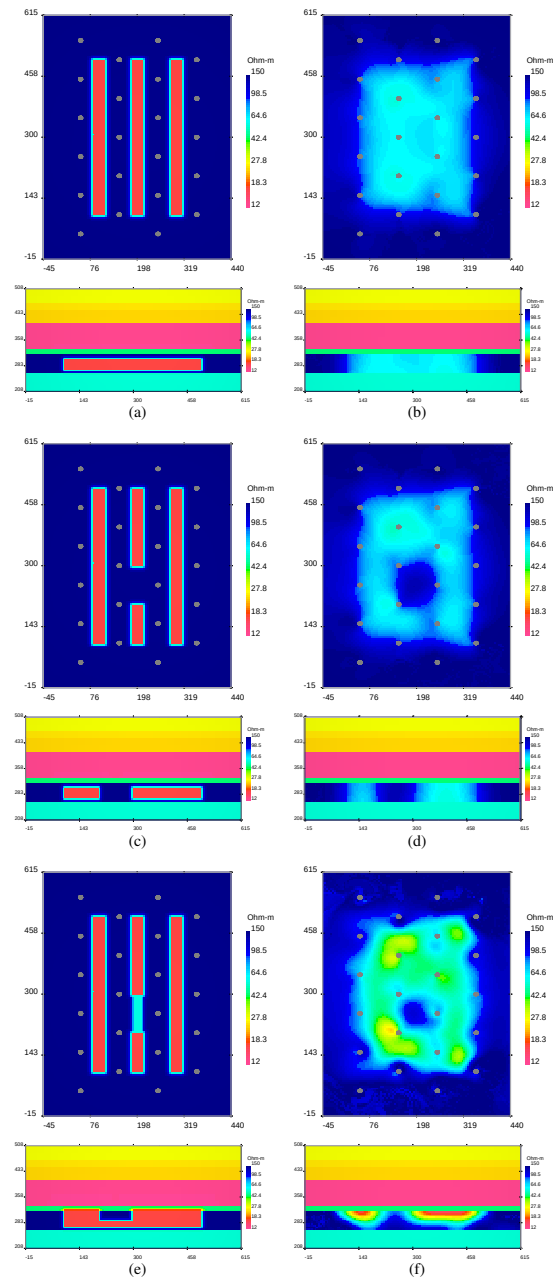

Figure 5: Each panel shows a plan-view of the models at z = 293 m and a cross-section at 200 m in the easting direction. Grey dots indicate the observation well locations that contain the borehole receivers. (a) True model with 3 regular steam chambers. (b) Recovered model showing the 3 regular steam chambers. (c) True model where the center chamber has impeded growth. (d) Recovered model indicating the impeded growth in the center chamber. (e) True model at a later time step, where the center chamber is impeded due to a blockage. (f) Recovered model using (d) as the initial model in time-lapse cascaded inversion. The model shows the grown chambers as well as the impeded area.

DOI http://dx.doi.org/10.1190/segam2015-5909921.1

EDITED REFERENCES

Note: This reference list is a copyedited version of the reference list submitted by the author. Reference lists for the 2015 SEG Technical Program Expanded Abstracts have been copyedited so that references provided with the online metadata for each paper will achieve a high degree of linking to cited sources that appear on the Web.

REFERENCES

Bell, J., A. Boateng, O. Olawale, and D. Roberts, 2011, The influence of fabric arrangement on oil sand samples from the Estuarine depositional environment of the Upper McMurray Formation: Presented at the AAPG International Conference and Exhibition.

Butler, R. M., 1994, Steam-assisted gravity drainage: Concept, development, performance and future: Journal of Canadian Petroleum Technology, **33**, no. 02, 44–50. http://dx.doi.org/10.2118/94-02-05.

Dembicki, E. A., 2001, The challenges in delineating Suncor's firebag in-sity oil sands project: Presented at the Canadian Society of Petroleum Geologists Rock the Foundation Convention.

Devriese, S. G. R., and D. W. Oldenburg, 2014, Enhanced imaging of SAGD steam chambers using broadband electromagnetic surveying: Presented at the 84th Annual International Meeting, SEG. http://dx.doi.org/10.1190/segam2014-1247.1.

Devriese, S. G. R., and D. W. Oldenburg, 2015, Imaging SAGD steam chambers: traditional ERT versus broadband electromagnetic methods: CSEG Recorder, **40**, 16–20.

Engelmark, F., 2007, Time-lapse monitoring of steam-assisted gravity drainage (SAGD) of heavy oil using multi-transient electromagnetics (MTEM): Presented at the CSPG CSEG Convention.

Haber, E., J. Granek, D. Marchant, E. Holtham, D. Oldenburg, and R. Shekhtman, 2012, 3D inversion of DC/IP data using adaptive OcTree meshes: Presented at the 82nd Annual International Meeting, SEG.

Hayley, K., A. Pidlisecky, and L. R. Bentley, 2011, Simultaneous time-lapse electrical resistivity inversion: Journal of Applied Geophysics, **75**, no. 2, 401–411. http://dx.doi.org/10.1016/j.jappgeo.2011.06.035.

Imperial Oil Resources Ventures Limited, 2013, Application for approval of the Aspen Project: Technical Report Volume 1.

Mansure, A. J., R. F. Meldau, and H. V. Weyland, 1993, Field examples of electrical resistivity changes during steamflooding: SPE Formation Evaluation, **8**, no. 01, 57–64. http://dx.doi.org/10.2118/20539-PA.

Reis, J. C., 1992, A steam-assisted gravity drainage model for tar sands: Linear geometry: Journal of Canadian Petroleum Technology, **31**, no. 10, 14–20. http://dx.doi.org/10.2118/92-10-01.

Singhal, A. K., and C. C. Card, 1988, Monitoring of steam simulation in McMurray Formation, Athabasca Deposti, Alberta: Journal of Petroleum Technology, **40**, no. 04, 483–490. http://dx.doi.org/10.2118/14215-PA.

Strobl, R., B. Jablonski, and M. Fustic, 2013, Opportunities and challenges in acessing stranded pay and heterogenous reservoirs in SAGD Bitumen Projects: Presented at the GeoConvention — Integration.

Tøndel, R., H. Schutt, S. Dummong, A. Ducrocq, R. Godfrey, D. LaBrecque, L. Nutt, A. Campbell, and R. Rufino, 2014, Reservoir monitoring of steam-assisted gravity drainage using borehole measurements: Geophysical Prospecting, **62**, no. 4, 760–778. http://dx.doi.org/10.1111/1365-2478.12131.

Unsworth, M., 2005, New developments in conventional hydrocarbon exploration with electromagnetic methods: CSEG Recorder, **30**, 34–38.

Waxman, M. H., and L. J. M. Smits, 1968, Electrical conductivities in oil-bearing shaly sands: SPE Journal, **8**, no. 02, 107–122. http://dx.doi.org/10.2118/1863-A.

Waxman, M. H., and E. C. Thomas, 1974, Electrical conductivities in shaly sands — I: The relation between hydrocarbon saturation and resisitivity index: II: The temperature coefficient of electrical conductivity: Journal of Petroleum Technology, **26**, no. 02, 213–225. http://dx.doi.org/10.2118/4094-PA.

Wynne, D. A., M. Attalla, T. Berezniuk, M. Brulotte, D. K. Cotterill, R. Strobl, and D. Wightman, 1994, Athabasca oil sands data McMurray/Wabiskaw oil sands deposit — Electronic data: Technical report, Alberta Geologic Survey.

Zhang, W., S. Youn, and Q. Doan, 2007, Understanding reservoir architectures and steam-chamber growth at Christina Lake, Alberta, by using 4D seismic and crosswell seismic imaging: SPE Reservoir Evaluation & Engineering, **10**, no. 05, 446–452. http://dx.doi.org/10.2118/97808-PA.

DOI http://dx.doi.org/10.1190/segam2015-5909921.1